

Intergranular fracture in 13 wt% chromium martensitic stainless steel

S. K. BHAMBRI

Fracture Mechanics and Fatigue, Corporate Research and Development Division, Bharat Heavy Electricals Limited, Hyderabad, India

Fracture of 13 wt% chromium steel blades has been observed to occur in the intergranular mode in certain service failures. An attempt has been made in this study to identify the conditions in respect of material, loading and environment which may lead to intergranular fracture. Three different materials were subjected to varying heat treatments selected on the basis of fracture characteristics of as-received materials. It has been concluded that grain-boundary segregations of impurities and carbide precipitation, intergranular network of delta ferrite at prior austenitic grain boundaries, and a sufficient concentration of NaCl in conjunction with cyclic stress, promote intergranular fracture in a 13 wt% chromium steel.

1. Introduction

The 13 wt% chromium martensitic stainless steels are a well established material for applications in steam turbines, marine turbines, compressor blades, and boiler feed pump shafts. For elevated temperature applications molybdenum and vanadium are generally added to 13 wt% chromium steel to impart heat-resistant properties. In addition to these elements, other elements such as niobium [1], niobium plus nitrogen [2] and tantalum plus nitrogen [3] are added to raise the strength level of this steel for applications in steam turbine rotors, particularly of higher rating plants. In all these applications 13 wt% chromium steel and its modified grades are employed in the hardened and tempered conditions.

Two grades of straight 13 wt% chromium steels are commonly employed in steam turbine bladings, i.e. one with 0.12 wt% carbon and the other with 0.2 wt% carbon. The selection of carbon level is made on the basis of the operational stresses experienced in service by the blading stages - 0.12 wt% carbon grade being selected for low stress levels in moving blades and in guide blades.

Some blade failures have been observed in steam turbines. Fractographic examination of the fracture surfaces of the failed blades in the scanning electron microscope has revealed an intergranular mode of fracture in a few cases. Numerous causes are known to be responsible for intergranular fracture in 13 wt% chromium steels. Temper embrittlement resulting from tempering a hardened steel in the temperature range 450 to 575°C is known to result in intergranular fracture during impact [4] and fast fracture [5].

In a Ni-Cr-Mo marine steel, Jones [6] has shown that even cooling rates following normal tempering can result in grain-boundary segregations in which case fatigue crack growth characteristics have greater sensitivity than impact energy transition properties. Therefore, in the present studies, fracture mechanisms have been investigated for both impact and fatigue

fractures. Intergranular fracture during corrosion fatigue in a 3 wt% NaCl aqueous solution has been extensively reported, e.g. [7]. The effect, of small concentrations of NaCl on the fracture mode during fatigue, however, has not received much attention. In this study, therefore, the influence of smaller concentrations of NaCl aqueous solutions on the fracture mechanism of corrosion fatigue failures has also been studied. In addition, the effect of certain microstructural conditions such as the presence of delta-ferrite at the grain boundaries on fracture mechanisms has also been examined.

Doig *et al.* [8] have recently shown that stress corrosion cracking of 13 wt% chromium steels in an alkaline solution of NaOH results in intergranular fracture when material is tempered to a hardness level above 280 BHN. Therefore, in blading materials tempered to hardness levels below 270 BHN such stress corrosion cracking is not expected to occur. Stress corrosion studies, therefore, have not been included here. Similarly, hydrogen embrittlement due to high hydrogen concentrations in the material is well known to result in intergranular fracture with low impact values, and hence has not been considered here.

2. Experimental procedure

Three materials, A, B and C, investigated in the present study had chemical compositions and mechanical properties as given in Tables I and II, respectively. Of these, materials, A and B are of same grade, a 0.12% C-13% chromium steel but from two different suppliers and material C is a 0.2% C-13% Cr-Mo-V steel (all compositions in wt%).

In the first instance impact and fatigue fractures were examined for materials in the normal hardened and tempered conditions (1000°C, 1 h; 700°C, 5 h). Subsequently, materials were subjected to different heat treatments depending on the observations made on the above. The materials were subjected to the following heat-treatment conditions to introduce

TABLE I Typical chemical composition of materials investigated

Material	C	Mn	Si	S	P	Cr	Mo	V	Ni
A, B	0.12	0.44	0.25	0.012	0.015	12.2	0.04	0.016	0.44
C	0.22	0.42	0.35	0.01	0.02	13.0	0.42	0.22	0.42

different microstructures and to study their influence on the fracture mechanisms, identifying the conditions for an intergranular fracture.

Material A (0.12% C–13% Cr steel)

(a) aust. 1000°C, 1 h, air cooled, tempered 700°C, 5 h, air cooled

(b) aust. 1000°C, 1 h air cooled, tempered 700°C, 10 h, air cooled

(c) aust. 1000°C, 1 h, air cooled, tempered 700°C, 15 h, air cooled

(d) aust. 1000°C, 1 h, air cooled, tempered 550°C, 5 h, air cooled

(e) aust. 1000°C, 1 h, oil quenched, tempered 700°C, 5 h, oil quenched

Material B (0.12% C–13% Cr steel)

(a) aust. 1000°C, 1 h, air cooled, tempered 700°C, 5 h, air cooled

(b) aust. 1000°C, 1 h, air cooled, tempered 780°C, 5 h, air cooled

(c) aust. 1300°C, 1 h, air cooled

Material C (0.2% C–13% Cr–Mo–V steel)

(a) aust. 1000°C, 1 h, air cooled, tempered 700°C, 5 h, air cooled

(b) aust. 1000°C, 1 h, air cooled, tempered 800°C, 5 h, air cooled

(c) aust. 1000°C, 1 h, air cooled, tempered 535°C, 5 h, air cooled

(d) aust. 1000°C, 1 h, air cooled

(e) aust. 1000°C, 1 h, furnace cooled

2.1. Metallography

The microstructures of the materials in different heat-treated conditions were examined and some of the typical structures are presented in micrographs in Fig. 1.

2.2. Impact testing

Charpy V-notch impact tests were carried out at room temperature (25°C) as defined by the ASTM standard E 23 on an Instrumented Impact Testing Machine. Impact energy values obtained for different materials are given in Table III.

2.3. Fatigue testing

Fatigue tests were carried out on a rotary bending fatigue testing machine (a completely reversed cycle). Corrosion fatigue tests were carried out on a rotary bending fatigue testing machine of Carl-Schenck make at a frequency of 100 Hz.

2.4. Fractography

The fracture surfaces of all test samples were examined in a Cambridge Stereoscan 150 scanning electron microscope.

3. Results

3.1. Microstructure

The materials in different heat-treated conditions are found to be fully martensitic or martensite tempered to varying degrees except for the furnace-cooled material. The furnace-cooled specimens had a grain-boundary network of cementitic carbides in a ferritic matrix (Fig. 1e). Austenitizing at 1300°C resulted in formation of delta-ferrite at grain boundaries (Fig. 1f).

3.2. Fractography

3.2.1. Impact fracture

Impact fracture mechanisms observed in 13% chromium steels for various microstructural conditions are shown in Figs. 2 and 3. The salient features are given below.

In 700°C, 5 h tempered conditions, materials A, B and C showed different fracture modes. While fracture in B was in the ductile mode, A and C showed mixed ductile–brittle mode. The brittle fracture in A was in the intergranular mode occurring early during crack growth. On the other hand, C depicted cleavage, the transgranular brittle fracture mode. Increasing the tempering time to 10 h and 15 h at 700°C for A resulted in a significant decrease in intergranular fracture mode and its complete elimination, respectively. Oil quenching, both following austenitizing and tempering at 700°C, 5 h also resulted in a complete ductile fracture.

Specimens from B and C were tempered at 780 and 800°C, respectively, to examine whether coarsening of grain-boundary carbides would lead to grain-boundary separation. The fracture mode in both specimens was observed to be completely transgranular and the fracture surface had large shear lips indicating a ductile fracture.

Tempering treatment at 550°C for 5 h following hardening resulted in a complete intergranular fracture in both materials A and C.

Heat treatment of B involving austenitization at 1300°C followed by air cooling resulted in the formation of delta-ferrite at prior austenite grain boundaries. Their impact fractures indicated grain-boundary separation but the grain facets at high

TABLE II Mechanical properties of as-received materials

Material	Yield stress (MPa)	UTS (MPa)	Elongation (%)	Charpy impact toughness (J)	Hardness (BHN)
A	520	705	24	136	229
B	441	656	28	145	217
C	686	823	17.7	60	254

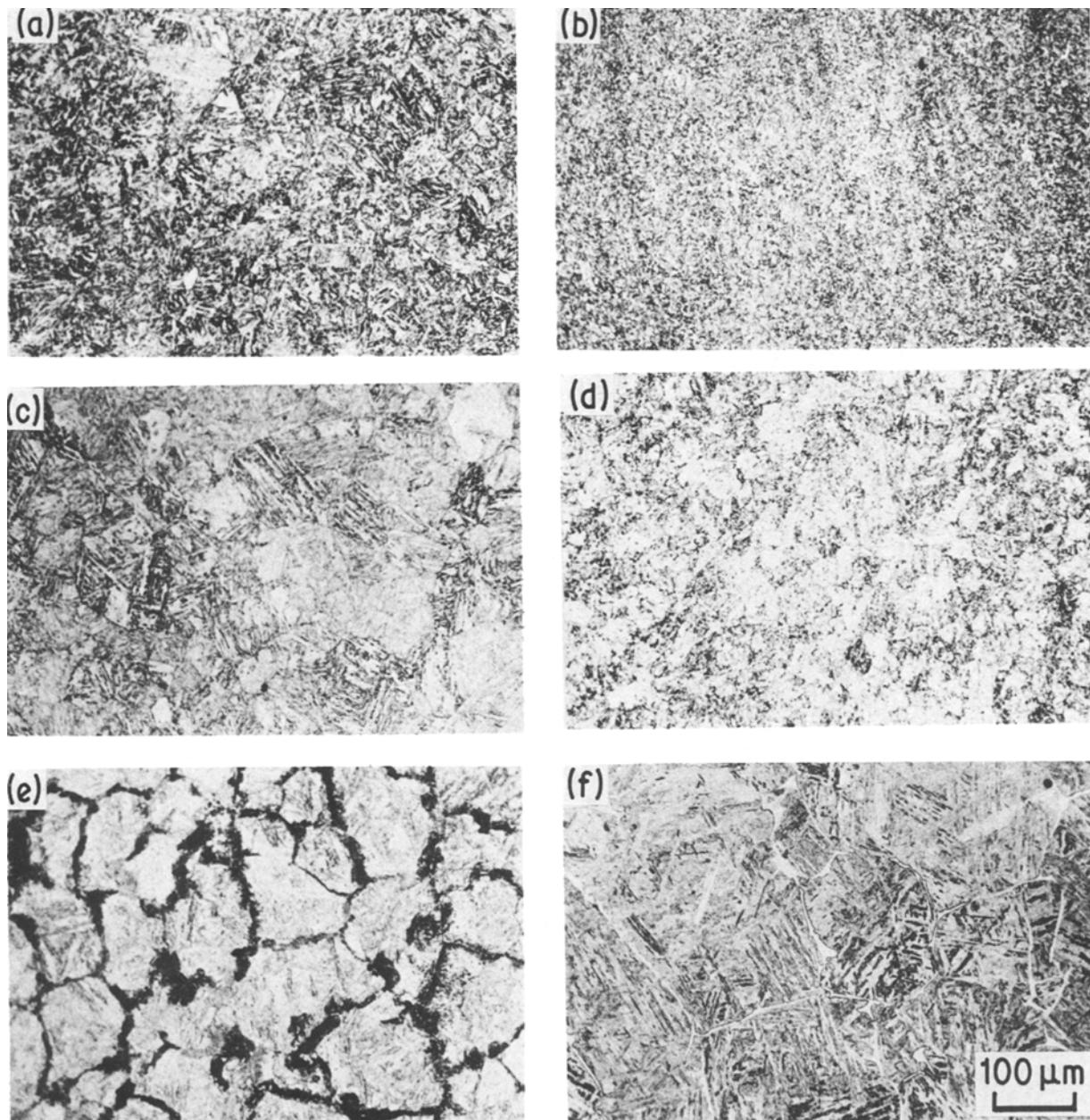


Figure 1 Microstructures introduced in 13% chromium steels through different heat-treatment cycles. (a) Tempered at 700° C, (b) tempered at 800° C, (c) tempered at 550° C, (d) air cooled from 1000° C, (e) furnace cooled from 1000° C, (f) air cooled from 1300° C.

TABLE III Effect of heat treatment on impact toughness

Material and heat treatment	Charpy impact (ISO-V notch) toughness (J)
<i>Material A</i>	
(a) 1000° C, 1 h; 700° C, 5 h	136
(b) 1000° C, 1 h; 700° C, 10 h	160
(c) 1000° C, 1 h; 700° C, 15 h	163
(d) 1000° C, 1 h; 550° C, 5 h	7
(e) 1000° C, 1 h, oil quenched; 700° C, 5 h, oil quenched	164
<i>Material B</i>	
(a) 1000° C, 1 h; 700° C, 5 h	145
(b) 1000° C, 1 h; 780° C, 5 h	158
(c) 1300° C, 1 h	7
<i>Material C</i>	
(a) 1000° C, 1 h; 700° C, 5 h	60
(b) 1000° C, 1 h; 800° C, 5 h	116
(c) 1000° C, 1 h; 535° C, 5 h	21
(d) 1000° C, 1 h, air cooled	14
(e) 1000° C, 1 h, furnace cooled	9

magnifications revealed “cleavage” and “dimple” mechanisms of fracture (Fig. 3b).

Impact fractures for microstructural conditions in material C resulting from cooling in the furnace or in air following austenitizing at 1000° C showed transgranular fractures in the cleavage and quasi-cleavage modes, respectively.

3.2.2. Fatigue fractures

Rotary bending fatigue fractures of specimens from materials A and B examined in the scanning electron microscope all revealed a transgranular mode of fatigue crack growth basically by the striation formation mechanism. The scanning electron micrograph in Fig. 4 represents the typical striation morphology.

In material C, the hardened and tempered structures showed a transgranular mode of crack propagation, striation formation and ductile tearing. In both the 700 and 800° C tempered specimens no intergranular fracture was observed. Intergranular facets

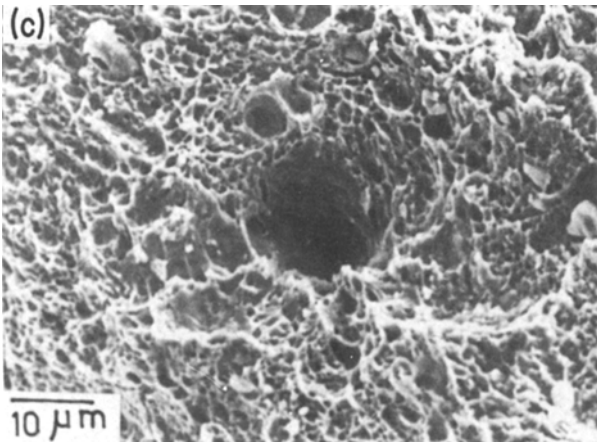
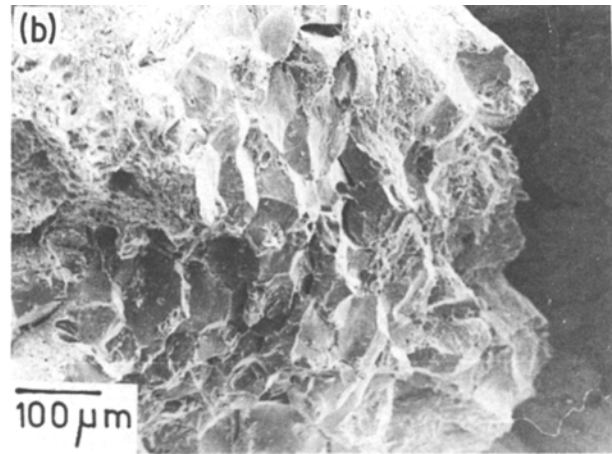
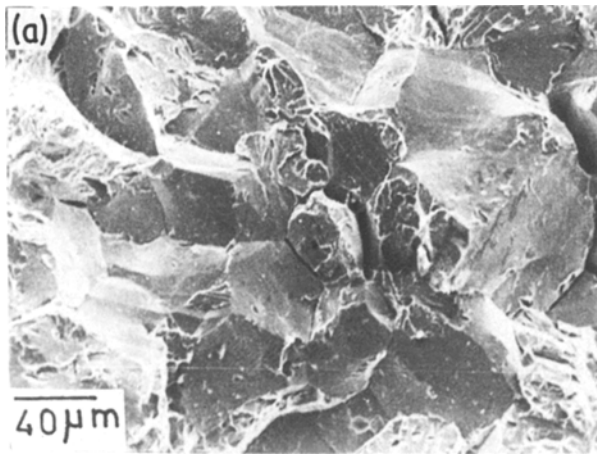


Figure 2 Scanning electron fractographs showing fracture mechanisms during impact failures in material A. (a) Intergranular fracture in material tempered at 700°C for 5 h, (b) small area of intergranular fracture after tempering for 10 h, (c) transgranular fracture in material tempered for 15 h.

was still observed, the crack propagation was primarily in a transgranular mode.

4. Discussion

4.1. Impact fractures

Normally in 13% chromium steels, hardened and tempered above 650°C, the impact fractures are observed to be transgranular [4]. Intergranular fracture observed in material A in a hardened and 700°C tempered condition is contrary to this as well as to the observed transgranular mode of fracture in materials B and C in similar heat-treated conditions. Such an anomalous fracture behaviour could arise from grain-boundary segregations of impurities which, however, simultaneously results in low impact toughness values. In contrast, the impact toughness value of 136 J is appreciably high. However, since grain-boundary segregations of impurity atoms can be reversed in 13% chromium steels, the material was subjected to different heat-treatment cycles to find whether grain-boundary segregation was the cause of intergranular component of the fracture process. With this objective in view the heat-treatment cycles were designed to retemper the material in the embrittlement reversal

appeared in the specimens cooled in air from the austenitizing temperature along with striations. In the furnace cooled specimen microcleavage was observed in addition to striations. The specimens from material tempered at 535°C showed a larger percentage of intergranular fracture in comparison with air-cooled specimen. A striation mechanism was also operative in this material as seen in Fig. 5.

Introduction of a corrosive environment, i.e. 1% NaCl aqueous solution, during fatigue resulted in the appearance of intergranular fracture along with a striation mechanism. However, a reduction in NaCl concentration reduced the intergranular part of fracture and at 0.01% NaCl concentration, though pitting

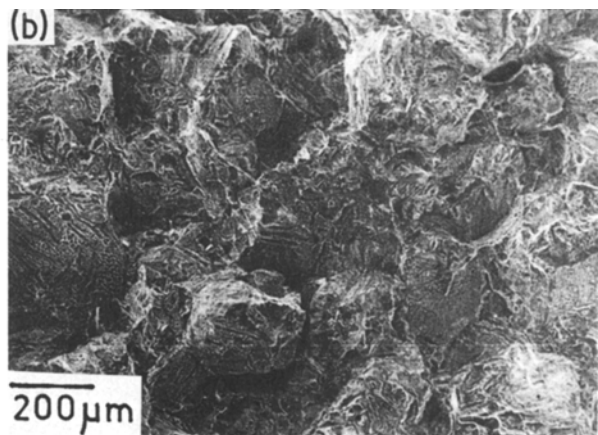
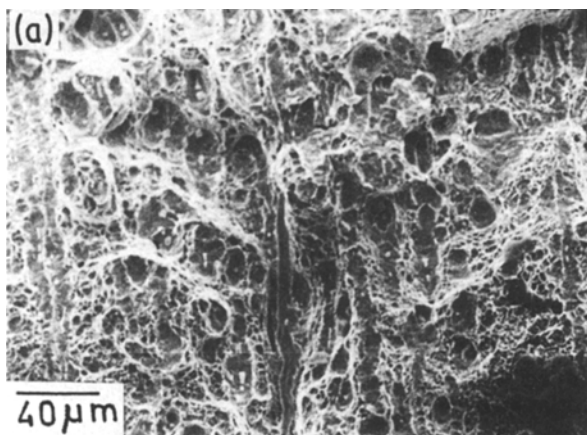


Figure 3 Fracture mechanisms operative in material B during impact fracture. (a) Transgranular fracture in material aust. 1000°C, 1 h and tempered at 700°C, 5 h; (b) intergranular fracture in material air cooled from 1300°C.

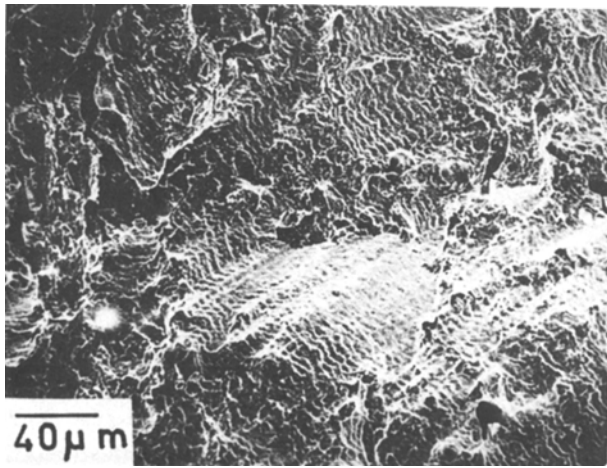


Figure 4 Typical fatigue fractures and striation morphology in 13% chromium steel.

range for prolonged durations and to increase the rate of cooling following austenizing and tempering treatments. Retempering at 700° C for further periods of 5 and 10 h resulted in a reduction in the intergranular fracture and its complete elimination, respectively, indicating this effect. This is further confirmed by the absence of intergranular fracture in an oil-quenched specimen. The role of grain-boundary segregation of trace elements [9] and carbide precipitation [10] in intergranular separation during impact fracture is now well established. Of the various impurity atoms (phosphorus, tin, manganese, silicon, etc.) phosphorus has been found to be particularly detrimental in 13% chromium steels [11]. Guillou *et al.* showed that in a 13% chromium steel, the phosphorus concentration at the grain boundary reached saturation only after 2 h tempering at 750° C. Another possible cause of intergranular fracture put forward by Prabhu Gaunker *et al.* [4] relates to depletion of carbon at grain boundaries due to precipitation of $M_7C_3 + M_{23}C_6 + M_2(C, N)$ carbides at martensite lath boundaries. This mechanism being responsible for intergranular fracture in material A in the present investigation is ruled out, or else intergranular fracture should also have been operative in material B which had a similar carbon content. The absence of intergranular fracture in the oil-quenched specimen tempered at 700° C further substantiates that carbon depletion at prior austenite grain boundaries is not the cause of intergranular fracture, since carbide precipitation in both air-cooled and oil-quenched specimens would be identical under similar tempered conditions. It is therefore concluded that a small amount of grain-boundary impurity segregation during air cooling is responsible for intergranular separation in material A.

Intergranular fracture observed in all materials A and C tempered at 535 or 550° C (in the embrittlement range) conforms to the reported fracture morphology. Prabhu Gaunker *et al.* [4] have shown that in 13% chromium steels the embrittlement begins at 450° C, reaches a maximum at 550° C and decreases further until 600° C when it disappears completely. M_7C_3 is the stable carbide in the temper embrittlement range and segregation of impurities on prior austenitic grain boundaries [9, 10] results in intergranular fracture in

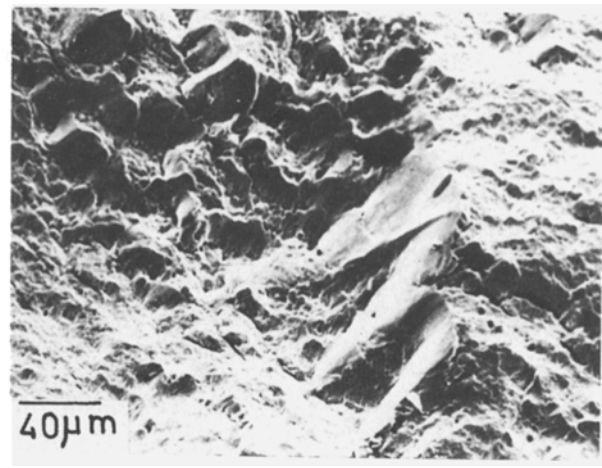


Figure 5 Intergranular facets appeared in material C tempered at 535° C during fatigue in air.

this microstructural condition. The presence of delta-ferrite at prior austenite grain boundaries in material B heat treated at 1300° C resulted in an intergranular separation during impact in a martensitic structure which otherwise shows a transgranular fracture. Delta-ferrite is richer in chromium, a ferrite stabilizer, than the matrix and is a brittle phase in comparison to the matrix [12]. Therefore, grain boundaries were weakened by the presence of delta-ferrite. To our knowledge, fracture morphology for 13% chromium steel in this microstructural condition has been studied for the first time in the present investigation. This result is of interest in many practical situations where 13% chromium steel components are welded.

The introduction of various microstructural conditions in material C through varying heat treatments has resulted in transgranular fracture during impact except when tempering was carried out in the embrittlement range. This indicates that any martensitic laths ending at grain boundaries do not promote an intergranular separation during impact. Similarly a preferential carbide precipitation and pearlite formation at prior austenite grain boundaries during furnace cooling does not result in an intergranular fracture. This is because of grain boundary strengthening by the cementitic carbide over a ferritic matrix.

4.2. Fatigue fracture

In all hardened and 700° C tempered A, B and C materials, the fatigue fractures were found to be transgranular with striation formation and ductile tearing. This is in contrast to impact fractures where intergranular fracture was observed in material A. An anomaly in fracture morphology is also noted for impact and fatigue fractures in material tempered in the embrittlement range. In this case, while impact fracture was completely intergranular, the fatigue fracture was in a mixed mode with transgranular striations and intergranular facets. On the other hand, intergranular facets appeared during fatigue crack propagation in a martensitic structure whereas the impact fracture in this microstructural condition was completely transgranular. The appearance of intergranular facets during fatigue in martensitic structure has also been reported by Kobayashi *et al.* [14], Lui

and Le May [15], and Crooker *et al.* [16]. The intergranular facets are found to decrease with the degree of tempering of martensite [15] until they completely disappear. The absence of intergranular facets in a 700°C tempered structure in the present study conforms to this. These observations are, however, contrary to the results reported by Ishii *et al.* [7] wherein a material tempered at 450°C did not show intergranular facets whereas fatigue fractures of materials tempered at 600 and 750°C revealed intergranular facets. The occurrence of intergranular fracture with striations during fatigue crack propagation in a material tempered at 535°C is analogous to that observed in a martensitic structure.

The appearance of intergranular facets in fatigue fractures in martensitic structure and in 535°C tempered structure can be attributed to ease in fracture along grain boundaries due to dislocation pile ups at grain boundaries and impurity segregations weakening the grain boundaries. Cooke *et al.* [17] have postulated that intergranular fracture occurs when the crack tip plastic zone size equals the prior austenite grain size. In such a situation the grain boundaries act as barrier to dislocation motion and become sites for dislocation pile ups resulting in grain-boundary separation. While the fatigue fracture in intergranular mode observed in a material with grain-boundary embrittlement can be attributed to the ratio of crack tip plastic zone size to prior austenite grain size, its presence in a martensitic structure and absence in 700°C tempered structure cannot be interpreted from the view point of this ratio alone. The results of Ishii *et al.* [7] support this argument or else intergranular fracture should also have appeared in 450°C tempered material in their study on 13% chromium steel. It appears that relative properties of matrix, second-phase precipitates and grain boundaries play a significant role in addition to the ratio of plastic zone size to prior austenite grain boundaries in determining the fracture mode in fatigue.

4.3. Corrosion fatigue fracture

Fatigue crack growth was primarily in the transgranular mode in 1.0% NaCl aqueous solution, the intergranular fracture being only a small fraction of the fracture surface. Ishii *et al.* [7] have also reported a mixed mode of crack growth during fatigue of 13% chromium steel in a 3% NaCl aqueous solution. Reduction in the NaCl concentration in the present study resulted in a decrease in the intergranular fracture proportion of the total fracture and at 0.01% NaCl level a completely transgranular fracture mode was operative. However, in this case pitting at successive crack front positions was observed in the slow crack growth regime. The reduction in aggressiveness of the corrodent resulted in slower near-threshold crack growth rates and with corrosion products in between the crack faces, the crack tip region acted like a crevice, resulting in pitting.

5. Conclusions

Fracture mechanisms operative during impact and fatigue fractures in the 13% chromium class of steels

have been studied for different conditions and the following conclusions have been drawn.

1. In the microstructural condition normally employed in steam turbine blading, impact fractures may occur in the intergranular mode in the presence of small concentrations of impurity segregation at grain boundaries. The intergranular fracture can be suppressed by increasing cooling rates following reversal treatment.

2. A grain-boundary network of delta-ferrite resulted in an intergranular fracture during impact.

3. Microstructural condition influenced the appearance of intergranular facets during fatigue crack growth. Of the various microstructures introduced, materials with martensitic structure and grain-boundary embrittlement showed intergranular facets.

4. Intergranular facets appeared in the corrosion fatigue fractures when the NaCl concentration in aqueous solution exceeded 0.01%.

Acknowledgements

The author wishes to thank the General Manager, Corporate Research and Development, BHEL, for his permission to publish this paper. The author is grateful to Mr K. Rajanna, Mr K. Satyanarayana and Mr Y. Sitaramaiah for their assistance in experimental work.

References

1. I. M. PARK and I. FUJITA, *Trans. ISI J.* **21** (1981) B372.
2. C. J. BOYLE and D. L. NEWHOUSE, *Met. Prog.* **87** (1965) 61.
3. M. KAWAI, K. KAWAGUCHI, H. YOSHIDA, E. KANAZAWA and S. MITO, *Tetsu-to-Hogane* **61** (1975) 229.
4. G. V. PRABHU GAUNKER, A. M. HUNTZ and P. LACOMBE, *Met. Sci.* **14** (1980) 241.
5. S. K. CHAUDHURI and R. BROOK, *Int. J. Fract.* **12** (1976) 101.
6. B. F. JONES, *Int. J. Fatigue* October (1981) 167.
7. H. ISHII, Y. SAKAKIBARA and R. EBARA, *Met. Trans. A* **13A** (1982) 1521.
8. P. DOIG, D. J. CHASTELL and P. E. J. FLEWITT, *ibid.* **13A** (1982) 913.
9. C. J. McMAHON Jr, C. L. BRIANT and K. BANERJEE, *Fracture* **1** (1977) 363.
10. C. L. BRIANT and S. K. BANERJI, *Met. Trans. A* **10A** (1979) 1729.
11. R. GUILLOU, M. GUTTMANN and Ph. DUMOULIN, *Met. Sci.* **15** (1981) 63.
12. D. J. GOOCH, *ibid.* **16** (1982) 79.
13. J. Z. BRIGGS and T. D. PARKER, "The Super 12% Chromium Steels" (Climax Molybdenum Company, New York, 1965) p. 6.
14. H. KOBAYASHI, R. MARAKAMI and H. NAKZAWA, "Fracture Mechanics and Technology", Vol. 1, edited by G. C. Sih and C. L. Chow (Noordhoff, Alphen aan den Rijn, 1979) p. 205.
15. M. W. LUI and I. LeMAY, "Microstructural Science", Vol. 8 (Elsevier, New York, 1980) p. 341.
16. T. W. CROOKER, D. F. HASSON and G. R. YODER, ASTM STP 600, (American Society for Testing and Materials, Philadelphia, Pennsylvania, 1976) p. 205.
17. R. J. COOKE, P. E. IRVING, G. S. BOOTH and C. J. BEEVERS, *Eng. Frac. Mech.* **7** (1975) 69.

Received 22 February
and accepted 11 July 1985